International Journal of Research in Engineering and Applied Sciences(IJREAS)
Available online at http://euroasiapub.org/journals.php
Vol. 12 Issue 06, June- 2022
ISSN(O): 2249-3905, ISSN(P) : 2349-6525 | Impact Factor: 8.202 |
Thomson Reuters ID: L-5236-2015

Optimization of Process Parameters for the Production of Honge Bio-oil from Honge Seedcake through pyrolysis.

Sharan Shegedar*[a], C H Biradar[b 1]

[a]*Department of Mechanical Engineering, Sharnbasva University, Kalaburagi-585103, India.*
[b]*Department of Automobile Engineering,Poojya Doddappa Appa College of Engineering, Kalaburagi -585102, India*

Abstract

Renewable energy from non-edible biomass can help to meet rising energy demands while reducing pollution. In the present work, a continuous feed fluidized bed pyrolysis reactor used to convert the biomass waste (Honge seedcake) into Honge bio-oil (HBO) and investigates the optimal pyrolysis conditions for obtaining maximum HBO yield. The optimum process parameters were found by Taguchi method. The predicted HBO yield was 60.33 wt.%, but in the confirmation test the HBO yield was 59.80 wt.% observed when the reactor temperature was 525 °C, for a particle size below 300 microns, sweep gas flow rate of 7.5 LPM, and feed rate of 0.25 kg/hr. The percentage contribution of each process parameter was verified using the Analysis of variance (ANOVA) method and it is as follows: reactor temperature (73.38%) > particle size (12.80%) > sweep gas flow rate (11.34%) > biomass feed rate (2.48 %). Elemental analysis, Fourier Transform Infrared spectroscopy, and gas chromatography and mass spectroscopy analysis were used for the characterization of HBO. The calorific value (17.2MJ/kg) and elemental analysis revealed that it contains carbonaceous matter. FT–IR analysis indicated that the HBO contains hydroxyl, alkanes, carboxylic, and aromatic functional groups. Propionic acid (21.11 %), butane (3.59 %), 7-Tetradecene (3.58 %), 4-methylhexan-3-ol (2.80 %), and 2,2-Dimethoxybutane (2.67 %) were the majority of compounds discovered in a GC–MS analysis of the HBO. The results are consistent with previously published bio-oil values and the HBO may be useful as fuels and chemicals.

Keywords: Pyrolysis; Bio-oil; Characterization of bio-oil; Emulsions; Taguchi's design of experiment;

1. Introduction

Energy is most important and valuable for both developing and developed nations. Population growth, rapid urbanization, and industrialization are all rising energy demand. The main source of energy for meeting this demand is fossil fuels, and increased reliance on fossil fuels causes significant climate change. At the moment, fossil fuels (coal, oil and gas) account for roughly 85% of global energy demand [1]. According to BP statistics, global oil consumption accounts for approximately 33.05% of total global consumption [2]. The main

* Corresponding author. Tel.: +919480149888 ; fax: +918472277844.
E-mail address: sharan.shegedar@gmail.com

issues with the use of fossil fuels are that they are nonrenewable, finite in nature, detrimental to the environment, and expensive [3]. Renewable energy source like hydro, solar, wind, geothermal, and biomass energy accounts for 14% of global primary energy usage, of which 62% is biomass energy [4]. The biomass resources are renewable, widely available as waste on a local level, and a carbon-neutral energy source that contributes to meeting future energy demand in a sustainable manner. As a result, biomass is seen as a viable alternative to fossil fuels as a sustainable energy source.

Biomass is an organic substance obtained from plants and animals. The biomass can be used as an energy source and has the potential to contribute in meeting energy demands sustainably. Biomass resources that are locally available as a waste could be directly converted into biofuels using various methods. Thermo-chemical, bio-chemical, and physical methods are used for production of bio-fuels from biomass. Combustion, gasification, pyrolysis, and liquefaction are different kinds of thermo-chemical conversion. Among them pyrolysis process is the thermal cracking of biomass in an anaerobic atmosphere at elevated temperature to obtain valuable fuels and chemicals. The end products of pyrolysis of biomass are bio-oil (pyrolysis oil), bio-char, and gases. The proportion of end products and byproducts of pyrolysis mainly depends on several factors, including feedstock composition and process parameters. Pyrolysis has recently received considerable attention for producing liquid fuel because liquid fuel is easier to handle, store, transport, and use in automobiles, boilers, and turbines. It also tackle the problem of solid biomass waste management, which is otherwise costly and complex [4,5]. Research have been conducted to produce bio-oil and bio-char through pyrolysis of several kinds of biomass feedstock like wood, agricultural and forestry waste, sugar cane bagasse (a byproduct of the sugar industry), and nutshells [6]. Few studies were performed on pyrolysis of nonedible seedcake like Jatropha, Mahua and Neem to obtain bio-oil [7–9]. Oils derived from non-edible plants like Jatropha, Mahua, Honge (Karanja), Sea Mango, Jojoba, and others can be used to make biodiesel in India. Government of India (GOI) has undertaken a production of biodiesel strategy focused on Jatropha and Pongamia Pinnata oil-bearing seeds as a diesel substitute [10]. According to studies, seedcake produced during oil extraction via oil expellers could account for nearly 70% of the total weight of the seeds. The non-edible seedcakes basically contain toxic ingredients and unfit for human or animal consumption. Furthermore, direct disposal of these wastes causes issues such as environmental pollution caused by greenhouse gas (GHG) emissions and solid waste management [7]. It is critical to address toxic waste handling issues and convert it to valuable products through pyrolysis.

The GOI initiated a Honge tree plantation drive for local biofuel production in 2003. The availability of Honge seeds in India is currently calculated to be nearly 0.2 million metric tons (MMT) per year. The oil produced from Honge seeds using the mechanical oil expeller is nearly 30% of entire weight of the seed, leaving the remaining 70% of the seedcake as a byproduct [11]. This indicate that nearly 0.145 million metric tons of Honge seedcake (HSC)

International Journal of Research in Engineering and Applied Sciences(IJREAS)
Available online at http://euroasiapub.org/journals.php
Vol. 12 Issue 06, June- 2022
ISSN(O): 2249-3905, ISSN(P) : 2349-6525 | Impact Factor: 8.202 |
Thomson Reuters ID: L-5236-2015

will be generated per year. This massive quantity of seedcake generated during oil extraction must be dealt with efficiently and environmentally friendly. Hence, in the present work, HSC is used as a feed material for the pyrolysis process to generate pyrolysis oil (bio-oil) rather than simply discarding it as a waste.

The various pyrolysis process parameters like pyrolysis reactor set point temperature (RT), gas flow rate (GFR), feed particles size (PS), heating rate, feedstock feed rate (FR), type of biomass, and average condenser wall temperature affect the yield of pyrolysis products. The study on the Heinze retort fed with safflower demonstrated that biomass conversion via pyrolysis typically takes place at RT ranging from 400 to 700 °C and that when the RT is between 400 – 550 °C, the bio-oil yield increases, while at higher RT result in a decrease in bio-oil yield [12]. The RT has a notable impact on the production of pyrolysis products. At low temperatures (around 350 °C), a significant proportion of char could be produced, whereas, at higher temperatures above 700 °C, the majority of byproducts are non-condensable gases [13]. The majority of bio-oil products are produced at RT ranging from 450 to 550 °C. Furthermore, the studies have shown that the smaller feed particle sizes resulted in a significant increase in bio-oil output, heating rate, and GFR both affect the product yields [12]. The study reveals that there is limited information available on the influence of feed rate on the bio-oil yield through the pyrolysis process. Using HSC as a feedstock, Chandra Shekhar Singh et al.[14] studied the effect of process parameters such as RT, PS, and GFR on a fluidized bed pyrolysis reactor (FBR). The findings indicated that at optimized conditions such as RT 500 °C, PS of 0.99 mm, and GFR around 8 LPM, the highest bio-oil yield was around 65 wt.%. According to the findings, increasing the RT up to 500 °C increases the bio-oil as a result of improved heat transfer, which leads to adequate cracking of biomass and also releases greater amount of volatile matter from biomass. An increase in RT above 500 °C reduces production of bio-oil owing to cracking of volatile matter, which intern increases gas yield and lower the char formation. Larger PS and too small PS have detrimental impact on bio-oil production and moderate PS results in higher bio-oil production owing to adequate heat transfer. Rise in GFR up to 8 LPM results in increase in improved bio-oil production due to short residence time of volatile matter thus preventing secondary reactions. Similar observation was reported by Biradar et al.[7] using Jatropha seedcake as feedstock for FBR. However, many studies have been reported to understand the effect of process parameters on the pyrolysis to achieve optimal amount of bio-oil using various kinds of biomass [15]. In spite of the enormous amount of biomass pyrolysis studies presented in literature, the information gathered in the various studies is frequently contradictory, making it difficult to analyze the effect of the pyrolysis process parameters on bio-oil production. To clarify the influence of the pyrolysis process parameters on FBR using HSC as feedstock the Taguchi methodology was used with an objective of increasing the bio-oil yields at maximum level. The influence of the process parameters like RT, PS and GFR was investigated at different FR. Also the characterization of bio-oil produced at optimal process conditions is reported.

International Journal of Research in Engineering and Applied Sciences(IJREAS)
Available online at http://euroasiapub.org/journals.php
Vol. 12 Issue 06, June- 2022
ISSN(O): 2249-3905, ISSN(P) : 2349-6525 | Impact Factor: 8.202 |
Thomson Reuters ID: L-5236-2015

2. Materials and Methods

2.1.Preparation of HSC Biomass samples and characterization

Honge seedcake (HSC) was selected in the present work. HSC were collected from Gulbarga University, Gulbarga, India. The HSC was dried under natural sunlight for a day later the HSC was ground to using a domestic electric knife grinder into small particle size and sieved to a particle sizes of 100µm to 1000 µm using the sieve shaker. Then the Particles were sieved into three groups such as ≤ 300µm, 300-600µm, and 600-1000µm. Then these different ranges of the HSC particle sizes are used for the test runs (experiments) in the pyrolysis reactor for the bio-oil production. The HSC consist of consists of lignocellulose material and have varying composition of cellulose, hemicelluloses, lignin, lipids, and others [16]. The particle size in the range of 300µm- 600µm was selected for the characterization of HSC. The density of HSC was measured as 520 kg/m3. The proximate analysis (ASTM D3173-07) and elemenal analysis (ASTM D5291-96) were performed to characterize the HSC and check its suitability for pyrolysis process. The calorific value (CV) of selected HSC was measured with the help of bomb calorimeter and found to be 16.5 MJ/kg. The properties of HSC are mentioned in table 1.

Table 1. Properties of HSC.

Constituents (wt%)			Proximate analysis (% as-received)		Elemental analysis (% as-received)	
Hemicellulose[a]	31.2 ± 0.85		Moisture	9.64	Carbon	47.28
Cellulose[a]	27.6 ± 1.17		Volatile matters	71.55	Hydrogen	6.22
Lignin[a]	4.2 ± 0.51		Fixed carbon	13.3	Nitrogen	3.98
Lipid[a]	16.45 ± 1.13		Ash	5.51	Sulfur	0
others[a]	20.55		others	-	Oxygen*	42.52

a - [16] , *By difference

2.2 Experimental set up

The pictorial view of the lab-scale continuous feed pyrolysis reactor used for the present study is depicted in Fig. 1. Fig. 2 represents the schematic diagram of the experimental setup. The reactor consists of a cylindrical stainless steel tube (62.5 mm ID and 1.2m height) with ceramic surface heaters, a screw feeder, a cyclone separator, and a condenser. The reactor's heating section is divided into three zones, each 400mm long, with individual surface ceramic heating sections to heat the reactor. The three-zone heating system has the benefit of changing

International Journal of Research in Engineering and Applied Sciences(IJREAS)
Available online at http://euroasiapub.org/journals.php
Vol. 12 Issue 06, June- 2022
ISSN(O): 2249-3905, ISSN(P) : 2349-6525 | Impact Factor: 8.202 |
Thomson Reuters ID: L-5236-2015

the reactor heating length based on the requirements. The wall temperature and volatile gas temperature are measured using K-type thermocouples, and the reactor's wall temperature is adjusted and controlled by a temperature controller from the control panel. The N_2 gas flow meter regulates and helps to alter and control the vapour retention time in the reactor throughout the experiments. A screw feeder feeds HSC into the pyrolysis reactor, and feed rate will be adjusted and controlled by a variable frequency drive (VFD). Using VFD it can be possible to feed HSC to the pyrolysis reactor with a varying feed rate of 0.25kg/hr, 0.50kg/hr, and 0.75 kg/hr. The nitrogen (N2) gas cylinder and N_2 sweep gas pipeline consist of flow meter through which the gas flow rate to the reactor can be controlled. The sweep gas flow rate is measured in liter per minute (LPM).The reactor temperature can be controlled by temperature controllers during the pyrolysis and the evolved vapours are passed through a cyclone seperator to remove fine char particles carried in the gas stream. Then onwards vapours are carried to the condenser. The condensed vapour known as Honge bio-oil (HBO) was collected from the bottom of the condenser and the uncondensed gases were either collected or vented to the atmosphere. The type of condenser is water-cooled and made up of stainless steel (316LSS) tubing. The double pipe heat exchanger (single pass shell and tube with the counter-flow arrangement) is used as a condenser to quench hot vapours into bio-oil. The condenser wall temperature was kept at 16 °C by passing cold water through the outer tube (shell). The char formed during the pyrolysis process will be collected from the reactor's bottom and the cyclone separator. The bio-char may contain some ash as well as unaltered biomass. The bio-char produced could be used as an active carbon or as a fuel source, making it a valuable byproduct of the pyrolysis process. The collected HBO primarily composed of aromatic, oxygen compounds, aliphatic, and naphthenic hydrocarbons. Hence, it could be used as a value-added products (fuel) and chemicals. Furthermore, the uncondensed gas (pyro-gas) obtained through pyrolysis mainly contains CH_4, CO_2, CO, H_2, and lighter hydrocarbons which is flammable and can be used as fuel or for the synthesis of chemical compounds [17]. The percentage weight of HBO (Y_O) and percentage weight of bio-char (Y_C) are calculated using equations 1 and 2, respectively. The percentage weight of pyro-gas (Y_G) obtained is calculated by using equation 3.

$$Y_O = \frac{\text{Weight of HBO collected}}{\text{Weight of seedcake Supplied into the reactor } (W_B)} \times 100 \quad (1)$$

$$Y_C = \frac{\text{Weight of bio}-\text{char collected}}{\text{Weight of seedcake Supplied into the reactor } (W_B)} \times 100 \quad (2)$$

$$Y_G = 100 - (Y_o + Y_c) \quad (3)$$

Where, W_B is the weight of biomass (HSC) used for the pyrolysis process. Y_O, Y_C, and Y_G

International Journal of Research in Engineering and Applied Sciences(IJREAS)
Available online at http://euroasiapub.org/journals.php
Vol. 12 Issue 06, June- 2022
ISSN(O): 2249-3905, ISSN(P) : 2349-6525 | Impact Factor: 8.202 |
Thomson Reuters ID: L-5236-2015

are the percentage weights of HBO, bio-char, and Pyro-gas collected, respectively.

.

Fig. 1. Pictorial view of the continuous feed fluidised bed pyrolysis reactor.

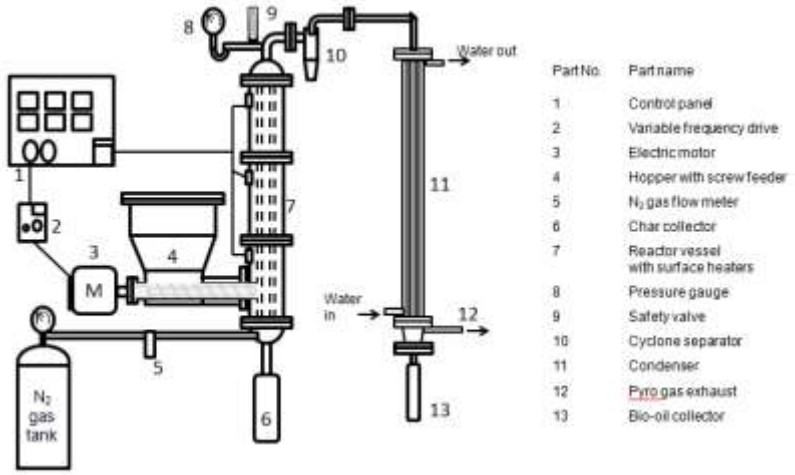

Part No.	Part name
1	Control panel
2	Variable frequency drive
3	Electric motor
4	Hopper with screw feeder
5	N_2 gas flow meter
6	Char collector
7	Reactor vessel with surface heaters
8	Pressure gauge
9	Safety valve
10	Cyclone separator
11	Condenser
12	Pyro gas exhaust
13	Bio-oil collector

Fig. 2. Schematic diagram of the experimental setup.

2.3 Taguchi design of experiment.

The four factors (process parameters) three level Taguchi's experimental design (DOE) technique was opted to find the influence of the process parameters on optimal bio-oil yield. Minitab-19 statistical software that includes Taguchi's L9 OA method is used in the present study. The process parameters evaluated include pyrolysis reaction temperature (RT), particle size (PS) of the feedstock, sweep gas (N_2 gas) flow rate (GFR), and HSC biomass feed rate

International Journal of Research in Engineering and Applied Sciences(IJREAS)
Available online at http://euroasiapub.org/journals.php
Vol. 12 Issue 06, June- 2022
ISSN(O): 2249-3905, ISSN(P) : 2349-6525 | Impact Factor: 8.202 |
Thomson Reuters ID: L-5236-2015

(FR), at a constant pyrolysis process reaction time of one and half hour. The purpose of this experiment is to maximize bio-oil yields. As a result, the larger the better approach of signal to noise (SNR) ratio was applied. The SNR ratio is given by the following equation 4.

$$SNR_i = -10\log\left(\frac{1}{n}\sum_{i=1}^{n}\frac{1}{(Y_i)^2}\right) \quad (4)$$

Here, 'n' denotes the number of experiments carried out and Y_i denotes the obtained bio-oil at i^{th} experiment. Four process parameters and three levels for the experiment of pyrolysis of HSC are summarized in the Table 2. The L9 orthogonal arrays (OA) that were built for analysis of bio-oil yields (Table3) and all the experiments are repeated for trice and average yield of bio-oil along with respective SNR are mentioned in the table 3.

Table 2. Four process parameters and three levels for HSC pyrolysis.

Process parameters	***Level 1***	***Level 2***	***Level 3***
RT	475 °C	525 °C	575 °C
PS	≤ 300 µm	300-600 µm	600-1000 µm
GFR	5 LPM	7.5 LPM	10 LPM
FR	0.25 kg/hr	0.50 kg/hr	0.75 kg/hr

Table 3. Experimental runs for Taguchi's L9 OA and measured bio-oil yield for HSC.

Run	***RT in °C***	***PS in µm***	***GFR in LPM***	***FR in kg/hr***	***HBO (Y_o) in wt. %***	***SNR***
1	475	≤ 300 µm	5	0.25	43.5	32.77
2	475	300-600 µm	7.5	0.5	44.9	33.04
3	475	600-1000 µm	10	0.75	38.6	31.73
4	525	≤ 300 µm	7.5	0.75	58.8	35.39
5	525	300-600 µm	10	0.25	53.5	34.57
6	525	600-1000 µm	5	0.5	44.3	32.93
7	575	≤ 300 µm	10	0.5	38.7	31.75
8	575	300-600 µm	5	0.75	27.2	28.69
9	575	600-1000 µm	7.5	0.25	33.1	30.40

International Journal of Research in Engineering and Applied Sciences(IJREAS)
Available online at http://euroasiapub.org/journals.php
Vol. 12 Issue 06, June- 2022
ISSN(O): 2249-3905, ISSN(P) : 2349-6525 | Impact Factor: 8.202 |
Thomson Reuters ID: L-5236-2015

2.4 Analysis of variance (ANOVA).

The present work targets to find the influence of process parameters on HBO yield by employing the ANOVA method. The ANOVA method is useful in evaluating the percentage contribution of each of process parameters considered for the study. ANOVA, like regression, is employed to analyse and model the connection among a "response variable and independent variables". ANOVA is useful for splitting the total sum of squares (SS_T) into process parameters that contribute to the responses used for the model, as well as the F-test is preferred for comparing the total deviation of the process parameters. The SS_T for an ANOVA with four process parameters at three different levels is given by the equation 5.

$$\text{Total sum of squares}, SS_T = \sum_{f=1}^{4} SS_f + SS_e \quad (5)$$

Here, SS_f represents the sum of square of the factor f, where f =1, 2, 3, and 4, here 1,2,3 and 4 indicates factor RT, PS, GFR, and FR respectively. The SSe represents the sum of squares error [18]. The commonly preferred parameter symbols in ANOVA are mentioned below. Total sum of squares (SS_T) from SNR is given by the equation 6.

$$SS_T = \sum_{i=1}^{n} (SNR)_i^2 - \frac{1}{n}\left[\sum_{i=1}^{n} (SNR)_i\right]^2 \quad (6)$$

Where, n is the number of tests conducted. The factors sum of squares (SS_f) can be determined as,

$$\text{Factors sum of squares}, SS_f = \sum_{j=1}^{r} \frac{[(SNR)_i]^2}{r} - \frac{1}{n}\left[\sum_{i=1}^{n} (SNR)_i\right]^2 \quad (7)$$

Here, 'f' represents the factors (tested), 'j' is the level of the specific factor f, 'r' is the repetition of each level of factor f.

The degree of freedom (DOF) is the number of independent comparisons that can be made in data. DOF for each control factor (D_f) is given by equation 8 and total DOF (D_T) is given by equation 9. The DOF for the error is difference of D_T and D_f.

$$\text{DOF of factor}, D_f = \text{No. of levels} - 1 \quad (8)$$

$$\text{Total DOF}, D_T = \text{Total No. of runs} - 1 \quad (9)$$

International Journal of Research in Engineering and Applied Sciences(IJREAS)
Available online at http://euroasiapub.org/journals.php
Vol. 12 Issue 06, June- 2022
ISSN(O): 2249-3905, ISSN(P) : 2349-6525 | Impact Factor: 8.202 |
Thomson Reuters ID: L-5236-2015

F-test for variance comparison (F_f) is the ratio of SS_f to the error or pooled error (S_e), and is employed to find which process parameter has a notable influence and is given by the equation 10 [18].

$$F_f = \frac{SS_f}{S_e} \quad (10)$$

The contribution (%) to the total variation is given by equation 11.

$$P_f(\%) = \frac{SS_f}{SS_T} \times 100 \quad (11)$$

Where, P_f indicates the total variance (%) of each individual factor.

2.5 *Characterization of the HBO*.

The dark brown HBO produced from pyrolysis of HSC at the optimal operation condition is collected and stored in an air tight bottle in the room maintained at an average temperature of 27 °C (Fig.3) and thereafter used for the test for characterization. The density, viscosity, calorific value, ash content, and elemental compositions have been found as per standards of ASTM. The chemical compounds and functional groups of the HBO were determined by gas chromatography–mass spectrometry (GC/MS) analysis and Fourier transform infrared spectroscopy (FTIR) methods respectively. The density of HBO was measured using hydrometer as per ASTM D1298 and found to be of 1078 kg/m3. Hamco (model: 48H1) capillary viscometer is used to measure kinematic viscosity of the HBO as per ASTM D445 and found to be 28 mm2/s. The calorific value (CV) of the HBO was measured with the bomb calorimeter (Sun Lab Tech Equipment, India) as per ASTM D240. The CV of HBO was found to be 17.2 MJ/kg. Thermo scientific (FLASH 2000) elemental analyser was considered to find the percentage compositions of Carbon (C), Hydrogen (H), and Nitrogen (N) in the HBO obtained at optimal pyrolysis process conditions. The amount of oxygen present in the HBO was determined by difference. An FTIR analysis identifies the various functional groups exist in the HBO. The Agilent Cary 630 FTIR spectrometer employed for the analysis of functional groups. SHIMADZU GCMS-QP2010 model with a Helium carrier gas flow rate of 1 ml/min used to detect various chemical compounds present in the HBO sample.

International Journal of Research in Engineering and Applied Sciences(IJREAS)
Available online at http://euroasiapub.org/journals.php
Vol. 12 Issue 06, June- 2022
ISSN(O): 2249-3905, ISSN(P) : 2349-6525 | Impact Factor: 8.202 |
Thomson Reuters ID: L-5236-2015

Fig. 3. Honge bio-oil (HBO).

3 Results and discussions

3.1 Analysis of variance (ANOVA)

The aim of the present work is to maximize the HBO yield under optimal conditions. Therefore the larger is the better SNR model was selected. The average SNR for each process parameter level, delta and rank of process parameters were presented in the Table 4. Delta indicates difference in level of highest to lowest SNR for individual process parameters and ranks of the process parameters are based on the values of delta. Table 5 shows the influence of each process parameter on the optimal HBO yield as well as the contribution (%) of each process parameter to the HBO yield. In the current work, all DOF are utilized by each of the process parameters, leaving no details for error determination thus "error variance is equal to zero". Hence, the importance of individual process parameter could be evaluated from the comparison of process parameter variances. Here, variance for FR was the lowest and considered as least influencing (insignificant). Due to the fact, both variance as well as the DOF of FR were pooled into error to calculate error variance [18]. It was realized from Table 5, that the calculated values for RT, PS and GFR were detected to be greater than FR. The highest F_f values were calculated for RT, PS, and GFR, which were the most influential process parameters. The calculated FR values is found to be lower, represents FR is statistically don't have significant influence on the HBO yield. The process parameters which affected the SNR values are depicted in the Fig.4, which helps to understand the related contributions of the numerous levels of the process parameters

International Journal of Research in Engineering and Applied Sciences(IJREAS)
Available online at http://euroasiapub.org/journals.php
Vol. 12 Issue 06, June- 2022
ISSN(O): 2249-3905, ISSN(P) : 2349-6525 | Impact Factor: 8.202 |
Thomson Reuters ID: L-5236-2015

Table 4. Response Table for Signal to Noise Ratios for larger is the better.

Level	RT	PS	GFR	FR
1	32.52	33.3	31.46	32.58
2	34.29	32.1	32.94	32.58
3	30.28	31.69	32.68	31.94
Delta	4.01	1.62	1.48	0.64
Rank	1	2	3	4

Table 5. Results of ANOVA with pooled error.

Process parameters	Sum of Squares (SS)	DOF	Adj. mean squares (Adj MS)	Variance ratio (F_f)	% contribution of process parameter towards response	Remark
RT	24.2664	2	12.1332	29.63	73.38	significant
PS	4.2385	2	2.1193	5.17	12.80	significant
GFR	3.7486	2	1.8743	4.58	11.34	significant
FR	0.8189	2	0.4095	1	2.48	insignificant
Error	0	0	-	-	-	-
Total	33.0724	8	16.5363	-	-	-
Pooled error	0.8189	2	0.4095	-	-	-

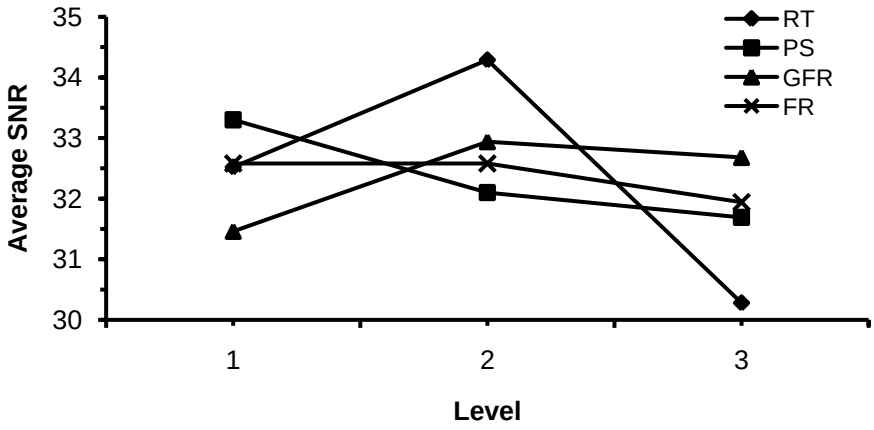

Fig. 4. SNR averages against Level for HBO yield.

on the optimal HBO yield. From Fig. 4 it can be seen that the optimum process parameters for the HBO yield were identified as RT at level 2 (525 °C), PS at level 1 (below 300 micron), GFR at level 2 (7.5 LPM) and FR at level 1 (0.25 kg/hr). At these optimal conditions, the predicted yield was estimated was 60.33 wt. % and the confirmation experiment were carried out for the pyrolysis of HSC and obtained yield of bio-oil was found to be 59.80 wt.% which was close to the predicted yield. The percentage contribution of process parameters towards the HBO yield was calculated as shown in Table 5. The greater a process parameter's contribution to the overall variation indicates the greater its capacity to effect the SNR. The chosen particular process parameters in this work could be ranked according to their effects based on the F-test as well as the percentage contribution of process parameters against the optimal HBO yield in the following order: RT > PS > GFR > FR.

3.2 Influence of process parameters on HBO yields

3.2.1 Influence of RT on HBO yield

The operational conditions of pyrolysis process influence the HBO yield. The influence of RT, PS, GFR, and FR on pyrolysis of HSC to obtain HBO yield was studied. The HBO yield mainly relied on the pyrolysis RT as shown in Fig. 4 and Fig.5. The Mean of means against level for HBO response was observed in Fig. 5 as per Taguchi's L_9 experiments and at level 2 (525 °C) the HBO yield response was 52.2 wt. %. However the HBO yield decreased by 24.26 wt. % when RT is at 475 °C and 36.78 wt. % when RT at 575 °C. C.H. Biradar et al. [7] reported that the optimal yield of bio-oil obtained using Jatropha seedcake was 48 wt. % when RT was at 450 °C in a similar type of pyrolysis reactor. At the reactor core the maximum vapour (including carrier gas) temperature was nearly 25 °C lower than the RT under steady operating conditions. Thus, the vapour temperature at optimal condition is close to 500°C, which is the same as the situation observed by Bridgewater et al. [19] for optimal bio-oil yield in the FBR. The bio-oil yield dropped and the non-condensable gas yield rised, when the RT increased above 525°C. These may be because of the increased vapors cracking at the higher reaction temperature. The drop in the bio-oil yield at lower RT could be due to unconverted biomass feedstock mostly during pyrolysis at lower RT [20]. In the present study at optimal conditions, the predicted HBO yield estimated was 60.33 wt. % and in the confirmation experiment the obtained HBO yield was found to be 59.80 wt. % which is nearly matching to the predicted yield.

International Journal of Research in Engineering and Applied Sciences(IJREAS)
Available online at http://euroasiapub.org/journals.php
Vol. 12 Issue 06, June- 2022
ISSN(O): 2249-3905, ISSN(P) : 2349-6525 | Impact Factor: 8.202 |
Thomson Reuters ID: L-5236-2015

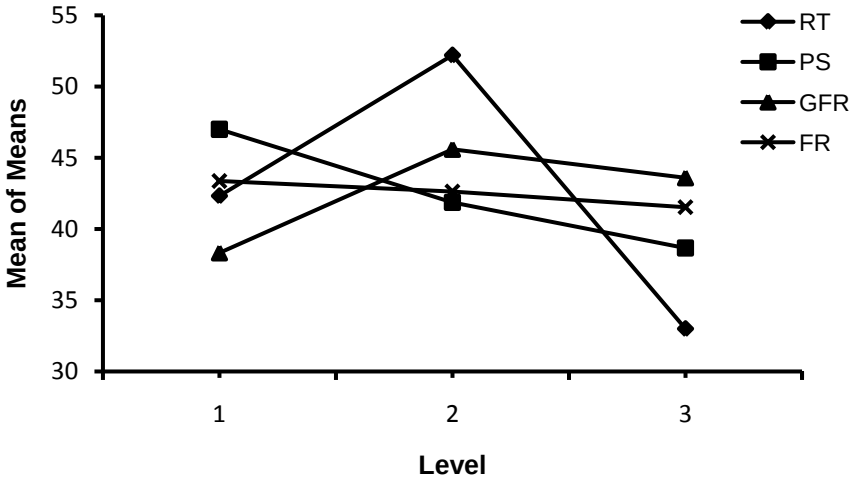

Fig.5. Mean of Means against Level for HBO yield.

3.2.2 Influence of PS on HBO yield

Studies have shown that yield of the bio-oil depends on the feed PS. Fig.5 shows the inverse effect of PS on the HBO yield. At lower PS increased HBO yield was observed. For PS at level 1 mean yield of HBO was 47 wt.% and followed a decreasing trend for level 2 (41.87 wt.%) and level 3 (38.67 wt.%). The inverse influence of PS on HBO yield can be attributed to the low thermal conductivity of the lignocellulosic materials, which is typically 0.1W/m^2 °C. As a result, the reduced PS provides more surface area as well as particles attain faster heating rate to complete pyrolysis within the available residence time, resulting in higher bio-oil yield [7]. On other hand, the heating rate of biomass particles decreases with increasing the PS. As the PS were increased, both the particle heating time and vapour escape time from the particles increases, which leads to increased char formation and reduced the bio-oil yield. Shen et. al.[21] observed that the production of bio-oil was highest for PS less than 300 microns. However, increasing the average PS from 300 micron to 1500 micron reduced the bio-oil yield significantly. This hypothesis backs up our findings, which show that as feed PS are reduced, bio-oil yield increases. Similar trends of inverse correlation among the production of bio-oil and feed PS have also been reported by Shen et. al.[21]. Shen et. al.[21] also discovered that using smaller biomass feedstock PS in the pyrolysis reactor results in decreased yields of lighter fractions compositions in the bio-oil and relatively increased yields of heavy fractions using large PS, which was verified with the use of GCMS study. From the results of ANOVA the influence of the PS on bio-oil production is statistically significant and optimum PS for the present work was considered below 300 μm.

International Journal of Research in Engineering and Applied Sciences(IJREAS)
Available online at http://euroasiapub.org/journals.php
Vol. 12 Issue 06, June- 2022
ISSN(O): 2249-3905, ISSN(P) : 2349-6525 | Impact Factor: 8.202 |
Thomson Reuters ID: L-5236-2015

3.2.3 Influence of GFR on HBO yield

The GFR is another vital process parameter in the pyrolysis. The effect of GFR on pyrolysis characteristics has rarely been presented in the literature. Some studies on pyrolysis reactors have revealed that increasing GFR increases HBO yield because vapours are carried out of the pyrolysis zone much before occurrence of secondary reactions, otherwise the vapours will be catalysed by char and further cracking of the vapours leads to non-condensable gases [22]. The production of bio-oil is found to be decreased as gas flow increases. This characteristic demonstrated that the higher flow rate of fluidization gas helped in the removal of vapours. Moreover, this process reduces contact time for both reactor and the condenser, resulting in a lower bio-oil yield [23]. Raja et al.[24], observed that the increased GFR during the pyrolysis of Jatropha seedcake in FBR from 20.83 to 29.17 LPM resulted in increased bio-oil quantity from 37.78 to 64.25 wt.%. Further increase in the GFR from 29.17 to 40 LPM reduced yield of bio-oil around 30.5 wt.%. Several researchers have examined the GFR in pyrolysis found that by increasing the flow of inert gas improves yield of bio-oil. However, increased GFR minimise bio-oil yield caused by incomplete condensation of vapours in the condenser, resulting in an increased gas yield, and portion of the unreacted feedstock can also be pushed out of the reactor even before pyrolysis is accomplished [15].

In the present study, the nitrogen GFR through the continuous feed fluidized bed pyrolysis reactor will significantly affect HBO yield as shown in the Fig. 5. For GFR at level 1 mean yield of HBO was 38.33 wt. %, at level 2 (45.6 wt. %) and at level 3 (43.6 wt. %). When the GFR is reduced to 5LPM, the HBO yield decreases because fluidization is not completely achieved, and the pyrolysis of feedstock may not occur completely. In addition to this, secondary reactions (cracking of volatile vapours) will take place as a result of the vapours longer retention time in the reactor. It was observed that, when the GFR was at 7.5 LPM, the improved fluidization in the pyrolysis zone aided in the rapid removal of vapours, resulting in minimal secondary reactions and maximum bio-oil yield (Fig.5). Further increasing the GFR above 7.5 LPM (i.e., around 10 LPM) results in a decrease in HBO yield from 45.6 to 43.6 wt. %. Increased GFR may reduce the contact time for of the vapours in the condenser, resulting in a lower HBO yield

3.2.4 Influence of FR on HBO yield

The influence of FR on bio-oil production was rarely described. The FR can influence the rate of heat transfer, fluidization characteristics, volatile matters (VM) retention time, and secondary reactions. Heat transfer is quicker at reduced FR, which not only contributes to faster pyrolysis, resulting in the formation of VM. However, the occurrence of VM is lower at slower feed rates than at quicker feed rates, and the retention time of VM is longer at slower feed rates. This indicates that the VM-char interaction seems to be much longer, which results

in VM's secondary reactions. The retention time of the VM is shorter at higher FR, so the secondary reaction of VM is reduced, and thus the bio-oil yield is higher [15]. According to Wu et al.[25] increasing the FR produces more condensable VM and reduces VM retention time inside the reactor system, which inhibits secondary reactions and contributes to a greater amount of bio-oil yield. Study of pyrolysis of sawdust in FBR revealed that the increase in FR from 3.5 to 4.0 kg/h resulted in increase of bio-oil yield from 62 to 63.5 wt.%. However, the increased FR (4.5–5.0 kg/h) reduced the yield of bio-oil because of the short retention time inside the reactr due to insufficient heating of feedstock particles. Another study revealed that as the FR increases, bio-oil production decreases because pyrolysis vapour motion may decrease, resulting in secondary reactions [26]. These findings are in consistent with the present study, which shows that as the FR increases the bio-oil yield decreases slightly (Fig. 5).

The results of influences of various process parameters on response of HBO indicate that the HBO yield improves with increasing RT, reaches a maximum yield of HBO at 525 °C, and then decreases with a further increase in RT as shown in Fig. 5. PS is the second most influencing parameter and the yield of HBO significantly improved with the reduction in PS (less than 300μm). The GFR significantly affects the yield of HBO and is improved with an increased GFR up to 7.5 LPM, further increasing the GFR (10 LPM) result in lower HBO yield and it may be attributed to less time for condensation. The FR of HSC is not much significant compared to other process parameters. From the Fig 4 and Fig. 5 it can be realized that at lower FR (approximately 0.25 kg/hr) allows better heat transfer of feedstock to reach pyrolysis temperature quickly and better thermal degradation of feedstock is possible releasing more amount of VM intern results in to higher HBO yield. The present results of influence of various process parameters are in broad agreement with the findings reported in the literatures [7,12,22].

3.2.5 Characterization of the HBO

Bio-oil is relatively unstable, acidic, high water content and a mixture of a oxygenated organic compounds. The bio-oil is a mix of aqueous phase (polar) and non-aqueous viscous phase (non-polar). The aqueous phase (polar) has organic compounds with low molecular weight, whereas the viscous phase (non-polar) contains oxygenates, aromatics, and polycyclic aromatic hydrocarbons with high molecular weight [27]. The density, viscosity, flash point, fire point, calorific value, and elemental analysis of HBO derived under the chosen optimal process parameters conditions were performed and compared with diesel (Table 6). Table 6 shows that HBO has a higher viscosity and oxygen content than diesel, but has a lower calorific value. The chemical compounds and functional groups of the HBO were determined by gas chromatography–mass spectrometry (GC-MS) and Fourier transform infrared spectroscopy (FTIR) techniques respectively. Bio-oil produced through pyrolysis usually has

International Journal of Research in Engineering and Applied Sciences(IJREAS)
Available online at http://euroasiapub.org/journals.php
Vol. 12 Issue 06, June- 2022
ISSN(O): 2249-3905, ISSN(P) : 2349-6525 | Impact Factor: 8.202 |
Thomson Reuters ID: L-5236-2015

significant amounts of several functional groups like aliphatic hydrocarbons, aromatic hydrocarbons, furans, amines, alcohols, acids, aldehydes, ketones, ethers, and esters [27]. Table 7 shows the GC–MS analysis of HBO, as well as the compounds with relative concentrations greater than 0.02%. Table 7 lists the sixty (60) chemical compounds found by HBO GCMS. From the Table 7, the most prevalent components are Propionic acid (21.11%), butane (3.59 %), 7-Tetradecene (3.58%), 4-methylhexan-3-ol (2.80 %), and 2,2-Dimethoxybutane (2.67 %). The GC-MS results display the presence of fatty acids, ethers, esters, hydrocarbons, and acids compounds, confirming that it could be used efficiently in the chemical, pharmaceutical and dyes industries, paint and perfume industries (Toluene) and biodiesel (ester and alkanes, toluene). Some of the chemical compounds determined by GC-MS are similar to those discovered by [28–30].

Table 6. Properties of the HBO obtained under optimal conditions.

Characteristics	HBO	Diesel
Appearance	Dark brown	Yellowish
Specific gravity	1.078	0.84
Kinematic viscosity @ 40 C in mm^2/s	28	2.7
Flash point °C	110	60
Fire point °C	130	65
GCV (MJ/kg)	17.2	42.5
Elemental analysis		
C	43	85.72
H	9.7	13.2
N	4.3	0.18
S	0.00	0.3
O* (by difference)	43	0.6

Table 7.GC–MS analysis of HBO.

S.No.	Compound	Formula	Area%	Retention time
1	Propionic acid	C3H5ClO2	21.11	1.053
2	Butane (n-Butane)	C4H10	3.59	1.109
3	Ethane, 1,1,1-trimethoxy-	C5H12O3	1.93	1.164
4	4-methylhexan-3-ol	C7H16O	2.80	1.216
5	Ethyl Acetate	C4H8O2	1.59	1.245
S.No.	Compound	Formula	Area%	Retention time
6	Butanoic acid, 1,1-dimethylethyl ester	C8H16O2	0.99	1.270
7	Acetone, dimethyl acetal	C5H12O2	1.75	1.330
8	Toluene	C7H8	1.11	1.354
9	Ether, 2-chloro-1-propyl isopropyl	C6H13ClO	1.08	1.416
10	2,2-Dimethoxybutane	C6H14O2	2.67	1.741
11	Benzeneacetamide	C8H9NO	1.08	1.809

International Journal of Research in Engineering and Applied Sciences(IJREAS)
Available online at http://euroasiapub.org/journals.php
Vol. 12 Issue 06, June- 2022
ISSN(O): 2249-3905, ISSN(P) : 2349-6525 | Impact Factor: 8.202 |
Thomson Reuters ID: L-5236-2015

12	2-Pentyne, 5-methoxy-	C6H10O	1.03	3.501
13	2-Butyne-1,4-diol	C4H6O2	1.00	4.520
14	1-Heptyn-4-ol	C7H12O	1.09	5.140
15	1,3-Methylene-d-arabitol	C6H12O5	1.03	5.910
16	4-(2)(Methylamino)ethyl)pyridine	C8H12N2	1.48	6.186
17	Pentanal	C5H10O	0.92	7.175
18	Cathine	C9H13NO	0.97	10.224
19	3-Octyn-2-ol	C8H14O	1.01	11.190
20	2-(5-Aminohexyl)furan	C10H17NO	0.87	12.511
21	Tetrakis(trimethylsiloxy)silane	C12H36O4 Si5	1.95	12.731
22	Phthalic acid, allyl ethyl ester	C13H14O4	2.12	14.345
23	Benzoic acid, 2,4-bis[(trimethylsilyl)oxy]-, trimethylsilyi ester	C16H30O4 Si3	2.11	15.178
24	2-Hexynoic acid	C6H8O2	1.11	15.555
25	2-methylbutyric acid	C5H10O2	0.98	15.680
26	Propionic acid amide	C3H7NO	1.11	15.765
27	Acetamide, N-(1-methylpropyl)-	C6H13NO	1.12	16.320
28	2-Furanethanol, á-methoxy-(S)-	C7H10O3	1.14	16.710
29	l-Gala-l-ido-octose	C8H16O8	1.02	16.795
30	Pentamethylene propionic acid	C11H18O3	1.35	16.880
31	Acetosyringone	C10H12O4	1.51	17.119
32	Propanamide, 2-methyl-	C4H9NO	1.03	17.335
33	Formic acid, chloro-, propyl ester	C4H7ClO2	0.87	17.505
34	Hexadecanoic acid	C9H18O2	1.32	18.223
35	keto-tri-hydroperoxides	C8H16O8	1.39	18.640
36	7-Hexadecenoic acid, methyl ester, (Z)-	C17H32O2	1.16	19.918
37	7-Tetradecene	C14H28	3.58	20.310
38	5-Butyltetrahydro-2-oxo-3-furancarboxilic acid	C9H14O4	1.31	20.550
39	3-Nonynoic acid	C9H14O2	1.17	21.480
40	Octadecane, 5-methyl-	C19H40	0.87	21.640
41	2-Propenamide, N-(1-cyclohexylethyl)-	C11H19NO	1.13	22.820
42	Arachidonic acid TMS	C23H40O2 Si	1.00	24.945
43	E-7-Tetradecenol,trimethylsilyl ether	C17H36OSi	1.06	26.735
44	1,2-Bis(trimethylsilyl)benzene	C12H22Si2	1.14	26.845
45	Tetradecanoic acid	C14H22O2	1.16	26.960
46	Thymol-TMS	C13H22OSi	1.23	28.115
47	Pentasiloxane, 1,1,3,3,5,5,7,7,9,9-decamethyl-	C10H32O4 Si5	0.98	28.665

International Journal of Research in Engineering and Applied Sciences(IJREAS)
Available online at http://euroasiapub.org/journals.php
Vol. 12 Issue 06, June- 2022
ISSN(O): 2249-3905, ISSN(P) : 2349-6525 | Impact Factor: 8.202 |
Thomson Reuters ID: L-5236-2015

48	6-Methyl-2-(3-nitrophenyl)imidazo[1,2-a]pyridine	C14H11N3O2	1.09	28.911
49	Benzoic acid, 3,5-dichloro-4-hydroxy-	C7H4Cl2O3	1.12	29.132
50	Luciduline	C13H21NO	1.11	29.355
51	Heptanedioic acid, 4-(ethoxycarbonylmethylene)-, diethyl ester	C15H24O6	1.18	29.475
52	1,2-Bis(trimethylsilyl)benzene	C12H22Si2	0.87	30.325
53	Arabinitol, pentaacetate	C15H22O10	1.45	30.578
54	1,4-Benzenedicarboxylic acid, bis(4-butylphenyl) ester	C28H30O4	1.22	31.021
S.No.	Compound	Formula	Area%	Retention time
55	Haloxazolam	C17H14BrFN2O2	0.97	31.875
56	N-Methyl-1-adamantaneacetamide	C13H21NO	1.89	32.104
57	Benzene, 2-[(tert-butyldimethylsilyl)oxy]-1-isopropyl-4-methyl-	C16H28OSi	1.20	32.315
58	Benzene, 1-(1,1-dimethylethyl)-4-(2-ethoxyethoxy)-	C14H22O2	0.92	33.120
59	3-Hydroxy-7,8-dihydro-.beta.-ionol	C13H20O2	0.97	33.606
60	Thiophene, 3,3'-(1,2-ethenediyl)	C10H8S2	1.02	34.335
		Total	100.00	

The FTIR analysis shows the functional groups exist in the HBO at wavenumber spanning from 4000-650 cm^{-1}, as depicted in Fig. 6. Table 8 lists the various functional group present in HBO using FTIR analysis. The

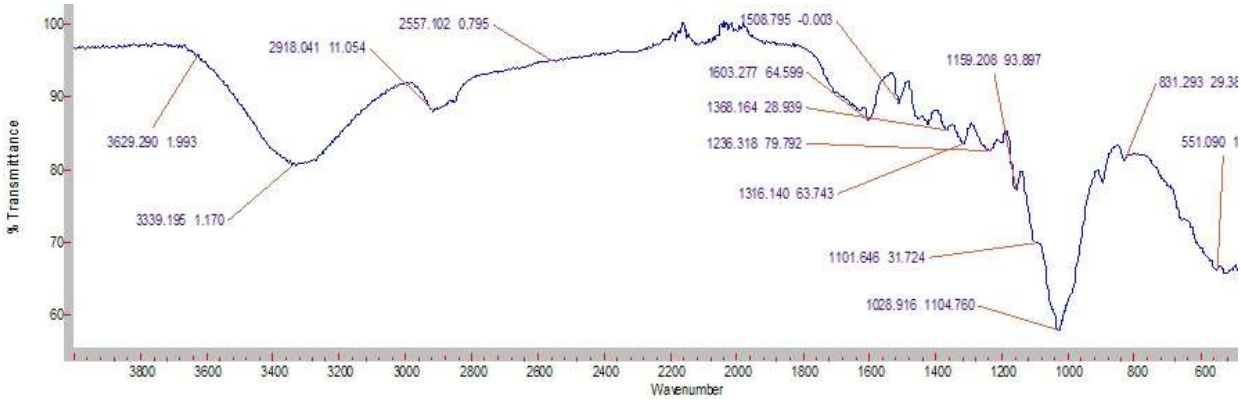

Fig. 6. FTIR Spectrum of HBO.

International Journal of Research in Engineering and Applied Sciences(IJREAS)
Available online at http://euroasiapub.org/journals.php
Vol. 12 Issue 06, June- 2022
ISSN(O): 2249-3905, ISSN(P) : 2349-6525 | Impact Factor: 8.202 |
Thomson Reuters ID: L-5236-2015

Table 8. Various functional groups present in the HBO using FTIR analysis.

Group	Molecular motion	Type of vibration	Intensity	Actual	Range
Alcohol	O-H	Strech, H-bonded	Strong, broad	3339.19	3200 - 3600
Alkanes	C-H	Stretch	Weak	2918.04	2850 - 3000
Alkynes	-C ≡ C-	Stretch	Variable	2153.9	2000 - 2270
Aldehydes Ketones	*C = O*	Stretch	Weak	1720.13	1700 - 1790
Alkenes	*C = C*	Stretch	Variable	1603.27	1600 - 1680
Aromatic	*C = C*	Stretch	Meduim	1508.79	1400 – 1600
Ether	C-O	Stretch	Strong	1236.31	1000 – 1300
Tertiary alcohol	C-O	Stretch	Strong	1158.20	1125 - 1200
Alkyl halide	C-Cl	Stretch	Weak	831	600 - 800
Alkenes	=*C*-H	Bending	Weak	631.3	675 - 1000

presence of wavenumber 3339.19 cm^{-1} between 3200 and 3600 cm^{-1} is related to the O-H stretching vibrations shows the existence of phenols, alcohols, and carboxylic acids. The narrow and weak bands occurrence in between 2850–3000 cm^{-1} refers to the C-H bonds, showing the existence of alkanes. The 2918.04 cm^{-1} wavenumber could be attributed to stretching vibrations of C-H bonds, indicating the presence of methanol and ethanol compounds in the HBO. The detected band at 2153.9 cm^{-1} reveals the C = C stretching vibration kind of alkynes compounds. The weak band at 1720.13 cm^{-1} is related to the carbonyl C=O stretching vibration indicating the presence of ketone and aldehyde groups [29]. The existence of C = C stretching vibrations at 1603.27 cm^{-1} and 1508.79 cm^{-1} shows evidence of alkenes and aromatic compounds, respectively. The band at 1236.31cm^{-1} shows the presence of ether (C-O). The large peaks in between 1050 and 1200 cm^{-1} indicate the C-O

stretching vibrations indicating the presence of primary, secondary, and tertiary alcohols. The band at 631.3 cm^{-1} exhibits the presence of =*C*-H bending vibrations from an alkene, whereas the wavenumber at 831 cm^{-1} exhibits the C-Cl stretching vibrations from an alkyl halide. Finally, the results of the FTIR analysis identify the indicating the presence of alkenes, alkanes, aromatics, and a variety of other chemical compounds like aldehydes, ketones, carboxylic acids, and phenols. Similar study with bio-oil has discovered the same majority of the functional groups[29,31].

4 Conclusions

The current study focuses on optimizing pyrolysis process parameters to obtain maximum HBO yield from pyrolysis of HSC in a continuous feed FBR using Taguchi Design of Experiments. The influence of chosen process parameters like RT, PS, GFR, and FR on HBO yield was investigated. According to the findings, the predicted yield of HBO at optimal operating conditions such as RT (525 °C), PS (less than 300), GFR (7.5 LPM), and FR (0.25 kg/hr.) was 60.33 %. The yield of HBO initially increases with increasing temperature, reaches an optimum at 525 °C, and then decreases with increasing temperature. The RT is the most influential process parameter, accounting for 73.38 % of the response (HBO yield), according to ANOVA. The PS appears to contribute 12.80% of HBO yield and is the second most significant process parameter in ensuring high HBO yield. The GFR is the third most important parameter, accounting for 11.34 % of the optimal HBO yield. However, when compared to other process parameters, FR has almost no effect on maximizing HBO yield. The HBO yield obtained in the confirmation test at optimal process parameters was 59.80 %, which was close to the predicted yield. The HBO's elemental analysis indicates that HBO is carbonaceous and has a slightly higher calorific value than its feedstock (HSC). Further. The HBO was analysed with FTIR and GCMS to determine the presence of various functional groups and chemical compounds. FTIR analysis revealed that the HBO contained functional groups such as amides, alcohols, alkenes, alkanes, aromatics, carboxylic acids, aldehydes, ketones, ethers, and esters. According to GCMS results, HBO is primarily a mixture of oxygenated aliphatic and aromatic hydrocarbon compounds ranging from C4 to C28. Hence, the findings support HBO as a promising candidate for use as a hydrocarbon fuel and chemical feedstock.

Reference

[1] Kober, T., Schiffer, H. W., Densing, M., and Panos, E., 2020, "Global Energy Perspectives to 2060 – WEC's World Energy Scenarios 2019," Energy Strateg. Rev., **31**, p. 100523.

[2] BP Statistical Review of World Energy 2020 1, 2020, "Statistical Review of World Energy 2020 | 69th Edition," bp.com, pp. 1–68 [Online]. Available:

https://www.bp.com/content/dam/bp/business-sites/en/global/corporate/pdfs/energy-economics/statistical-review/bp-stats-review-2020-full-report.pdf. [Accessed: 08-Dec-2021].

[3] Kalair, A., Abas, N., Saleem, M. S., Kalair, A. R., and Khan, N., 2021, "Role of Energy Storage Systems in Energy Transition from Fossil Fuels to Renewables," Energy Storage, **3**(1), p. e135.

[4] Hammani, H., El Achaby, M., El Harfi, K., El Mhammedi, M. A., Aboulkas, A., Jeguirim, M., and Khiari, B., 2020, "Optimization and Characterization of Bio-Oil and Biochar Production from Date Stone Pyrolysis Using Box–Behnken Experimental Design," Comptes Rendus. Chim., **23**(11–12), pp. 589–606.

[5] Jahirul, M. I., Rasul, M. G., Chowdhury, A. A., and Ashwath, N., 2012, "Biofuels Production through Biomass Pyrolysis —A Technological Review," Energies 2012, Vol. 5, Pages 4952-5001, **5**(12), pp. 4952–5001.

[6] Mohan, D., Pittman, C. U., and Steele, P. H., 2006, "Pyrolysis of Wood/Biomass for Bio-Oil: A Critical Review," Energy and Fuels, **20**(3), pp. 848–889.

[7] Biradar, C. H., Subramanian, K. A., and Dastidar, M. G., 2014, "Production and Fuel Quality Upgradation of Pyrolytic Bio-Oil from Jatropha Curcas de-Oiled Seed Cake," Fuel, **119**, pp. 81–89.

[8] Volli, V., and Singh, R. K., 2012, "Production of Bio-Oil from de-Oiled Cakes by Thermal Pyrolysis," Fuel, **96**, pp. 579–585.

[9] Pradhan, D., Bendu, H., Singh, R. K., and Murugan, S., 2017, "Mahua Seed Pyrolysis Oil Blends as an Alternative Fuel for Light-Duty Diesel Engines," Energy, **118**, pp. 600–612.

[10] Kumar, A., and Sharma, S., 2011, "Potential Non-Edible Oil Resources as Biodiesel Feedstock: An Indian Perspective," Renew. Sustain. Energy Rev., **15**(4), pp. 1791–1800.

[11] Muktham, R., Ball, A. S., Bhargava, S. K., and Bankupalli, S., 2016, "Study of Thermal Behavior of Deoiled Karanja Seed Cake Biomass: Thermogravimetric Analysis and Pyrolysis Kinetics," Energy Sci. Eng., **4**(1), pp. 86–95.

[12] Beis, S. H., Onay, Ö., and Koçkar, Ö. M., 2002, "Fixed-Bed Pyrolysis of Safflower Seed: Influence of Pyrolysis Parameters on Product Yields and Compositions," Renew. Energy, **26**(1), pp. 21–32.

[13] Chen, Y. C., Pan, Y. N., and Hsieh, K. H., 2011, "Process Optimization of Fast Pyrolysis Reactor for Converting Forestry Wastes into Bio-Oil with the Taguchi Method," Procedia Environ. Sci., **10**(PART B), pp. 1719–1725.

[14] Singh, C. S., Kumar, N., and Gautam, R., 2020, "Thermal Cracking of Karanja De-Oiled Seed Cake on Pyrolysis Reactor for Producing Bio-Oil with Focus on Its Application in Diesel Engine," IOP Conf. Ser. Mater. Sci. Eng., **804**(1), p. 012014.

[15] Guedes, R. E., Luna, A. S., and Torres, A. R., 2018, "Operating Parameters for Bio-Oil

Production in Biomass Pyrolysis: A Review," J. Anal. Appl. Pyrolysis, **129**, pp. 134–149.

[16] Jathanna, H. M., Rao, C. V., and Goveas, L. C., 2020, "Exploring Pongamia Seed Cake Hydrolysate as a Medium for Microbial Lipid Production by Aspergillus Ochraceus," Biocatal. Agric. Biotechnol., **24**, p. 101543.

[17] Morali, U., and Şensöz, S., 2015, "Pyrolysis of Hornbeam Shell (Carpinus Betulus L.) in a Fixed Bed Reactor: Characterization of Bio-Oil and Bio-Char," Fuel, **150**, pp. 672–678.

[18] Patel, S. R., and Murthy, Z. V. P., 2010, "Optimization of Process Parameters by Taguchi Method in the Recovery of Lactose from Whey Using Sonocrystallization," Cryst. Res. Technol., **45**(7), pp. 747–752.

[19] Bridgwater, A. V., Meier, D., and Radlein, D., 1999, "An Overview of Fast Pyrolysis of Biomass," Org. Geochem., **30**(12), pp. 1479–1493.

[20] Park, H. J., Park, Y. K., and Kim, J. S., 2008, "Influence of Reaction Conditions and the Char Separation System on the Production of Bio-Oil from Radiata Pine Sawdust by Fast Pyrolysis," Fuel Process. Technol., **89**(8), pp. 797–802.

[21] Shen, J., Wang, X. S., Garcia-Perez, M., Mourant, D., Rhodes, M. J., and Li, C. Z., 2009, "Effects of Particle Size on the Fast Pyrolysis of Oil Mallee Woody Biomass," Fuel, **88**(10), pp. 1810–1817.

[22] Onay, O., and Koçkar, O. M., 2006, "Pyrolysis of Rapeseed in a Free Fall Reactor for Production of Bio-Oil," Fuel, **85**(12–13), pp. 1921–1928.

[23] Heidari, A., Stahl, R., Younesi, H., Rashidi, A., Troeger, N., and Ghoreyshi, A. A., 2014, "Effect of Process Conditions on Product Yield and Composition of Fast Pyrolysis of Eucalyptus Grandis in Fluidized Bed Reactor," J. Ind. Eng. Chem., **20**(4), pp. 2594–2602.

[24] Raja, S. A., Kennedy, Z. R., Pillai, B. C., and Lee, C. L. R., 2010, "Flash Pyrolysis of Jatropha Oil Cake in Electrically Heated Fluidized Bed Reactor," Energy, **35**(7), pp. 2819–2823.

[25] Wu, S. R., Chang, C. C., Chang, Y. H., and Wan, H. P., 2016, "Comparison of Oil-Tea Shell and Douglas-Fir Sawdust for the Production of Bio-Oils and Chars in a Fluidized-Bed Fast Pyrolysis System," Fuel, **175**, pp. 57–63.

[26] Qureshi, K. M., Kay Lup, A. N., Khan, S., Abnisa, F., and Wan Daud, W. M. A., 2018, "A Technical Review on Semi-Continuous and Continuous Pyrolysis Process of Biomass to Bio-Oil," J. Anal. Appl. Pyrolysis, **131**, pp. 52–75.

[27] Banks, S. W., and Bridgwater, A. V., 2016, "Catalytic Fast Pyrolysis for Improved Liquid Quality," Handb. Biofuels Prod. Process. Technol. Second Ed., pp. 391–429.

[28] Bensidhom, G., Arabiourrutia, M., Ben Hassen Trabelsi, A., Cortazar, M., Ceylan, S., and Olazar, M., 2021, "Fast Pyrolysis of Date Palm Biomass Using Py-GCMS," J. Energy Inst., **99**, pp. 229–239.

[29] Chukwuneke, J. L., Orugba, H. O., Olisakwe, H. C., and Chikelu, P. O., 2021, "Pyrolysis of Pig-Hair in a Fixed Bed Reactor: Physico-Chemical Parameters of Bio-Oil," South African J. Chem. Eng., **38**, pp. 115–120.

[30] M. Azeez, A., Meier, D., Odermatt, J., and Willner, T., 2010, "Fast Pyrolysis of African and European Lignocellulosic Biomasses Using Py-GC/MS and Fluidized Bed Reactor," Energy & Fuels, **24**(3), pp. 2078–2085.

[31] Varma, A. K., Thakur, L. S., Shankar, R., and Mondal, P., 2019, "Pyrolysis of Wood Sawdust: Effects of Process Parameters on Products Yield and Characterization of Products," Waste Manag., **89**, pp. 224–235.